

UNIVERSITI MALAYSIA PAHANG

DECLARATION OF THESIS AND COPYRIGHT

Author's full name : Sabatanus Kait

Date of birth : 10 June 1993

Title : Effect Of Iron (Fe³⁺) doped Calcium Iron Copper Titanate
(CCTO)

Academic Session : Semester I 2016/2017

I declare that this thesis is classified as:

CONFIDENTIAL (Contains confidential information under the Official Secret Act 1972)

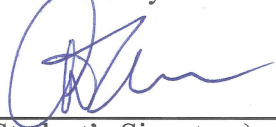
RESTRICTED (Contains restricted information as specified by the organization where research was done)

OPEN ACCESS I agree that my thesis to be published as online open access (Full text)

I acknowledge that Universiti Malaysia Pahang reserve the right as follows:

1. The Thesis is the Property of Universiti Malaysia Pahang
2. The Library of Universiti Malaysia Pahang has the right to make copies for the purpose of research only.
3. The Library has the right to make copies of the thesis for academic exchange.

Certified By:



(Student's Signature)

Sabastanus Kait
930610-12-5021

Date: 6/1/2017



(Supervisor's Signature)

Miss Mazni Binti Mustafa

Date: 6/1/2017

PERPUSTAKAAN UMP



0000119950

EFFECT OF IRON (Fe^{3+}) DOPED CALCIUM COPPER TITANATE OXIDE (CCTO)

SABASTANUS KAIT

Thesis submitted in fulfillment of the requirements
for the award of the degree of
Bachelor of Applied Science (Honor) Material Technology

Faculty of Industrial Sciences & Technology
UNIVERSITI MALAYSIA PAHANG

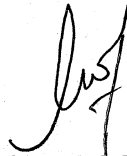
December 2016

PERPUSTAKAAN UNIVERSITI MALAYSIA PAHANG	
No. Perolehan 119950	No. Panggilan FST
Tarikh 12 OCT 2017	S23 2017 r ec.

SUPERVISORS' DECLARATION

I hereby declare that I have checked the thesis and in my opinion, this thesis is adequate in terms of scope and quality for the award of the degree of Bachelor of Applied Science (Honor) Material Technology.

Signature



Name of Supervisor

:

MISS MAZNI BINTI MUSTAFA

Position

:

SENIOR LECTURER


Date

:

08 DECEMBER 2016

STUDENT'S DECLARATION

I hereby declare that the work in this thesis is my own except for quotations and summaries which have been duly acknowledged. The thesis has not been accepted for any degree and is not concurrently submitted for award of other degree.

Signature : 
Name : SABASTANUS KAIT
ID Number : SC13010
Date : 08 DECEMBER 2016

DEDICATION

I dedicate this thesis to my family especially to my parent whose who help me unconditionally to finish this thesis.

ACKNOWLEDGEMENTS

Praise God for good health and wellbeing so that I could finish this thesis. I'm grateful to God for this opportunities and granting me successfully to finish this thesis.

First of all, I wish to express my sincere thanks to my supervisor Miss Mazni Binti Mustafa for providing ideas, suggestion and guidance step by step to complete this thesis. She also help me to find a suitable article and journal to read in order to complete this thesis. With her full support I manage to finish this thesis.

In addition, I would like to extend my sincere thanks to my group member for assist and gave an idea to complete this thesis. Furthermore, I would to express my sincere thanks to my laboratory assistant for providing all the necessary material and equipment to finish my laboratory works.

ABSTRACT

The $\text{CaCu}_3\text{Ti}_{4-x}\text{Fe}_x\text{O}_{12}$ ($x = 0, 0.05$ and 0.1) ceramics were synthesized by solid state reaction route and the microstructure and dielectric properties were studied. The X-Ray Diffraction (XRD) was used to analysis the lattice parameter and it was found that as the dopant contents increase the lattice parameter decrease. The microstructures were analyzed using Field Emission Scanning Electron Microscopy (FESEM) and it shows that as the dopant content increase the grain size increase. The dielectric measurement were performed at room temperature shows that with pure Calcium Copper Titanate (CCTO) doped with iron (Fe^{3+}), the dielectric permittivity (ϵ) at frequency 10 Hz decreases. Same goes with dielectric loss ($\tan \delta$), decrease when pure CCTO doped with iron (Fe^{3+}).

ABSTRAK

$\text{CaCu}_3\text{Ti}_{4-x}\text{Fe}_x\text{O}_{12}$ ($x = 0, 0.05$ dan 0.1) seramik telah disintesis melalui tindak balas dalam keadaan pepejal dan mikrostruktur dan sifat dielektrik telah dikaji. Pembelauan X-Ray (XRD) telah digunakan untuk menganalisis parameter kekisi dan didapati apabila kandungan pendopan meningkat maka parameter kekisi berkurangan. Mikrostruktur telah dianalisis dengan menggunakan Pelepasan Bidang Imbasan Mikroskop Electron (FESEM), dan telah menunjukkan bahawa apabila kandungan pendopan meningkat saiz butiran juga meningkat. Sementara itu pengukuran dielektrik telah dijalankan pada suhu bilik menunjukkan bahawa dengan Calcium Copper Titanate (CCTO) tulen didopkan dengan besi (Fe^{3+}), permittiviti dielektrik (ϵ) pada frekuensi 12 Hz berkurangan. Begitu juga dengan dielektrik loss ($\tan \delta$) menurun apabila CCTO tulen didopkan dengan besi (Fe^{3+}).

TABLE OF CONTENTS

	Page
	i
SUPERVISORS' DECLARATION	iii
STUDENT'S DECLARATION	iv
DEDICATION	v
ACKNOWLEDGEMENTS	vi
ABSTRACT	vii
ABSTRAK	viii
TABLE OF CONTENTS	ix
LIST OF TABLES	xiii
LIST OF FIGURES	xiii
LIST OF SYMBOLS	xiv
LIST OF ABBREVIATIONS	xv
CHAPTER 1 INTRODUCTION	1
1.1 BACKGROUND OF STUDY	1
1.2 PROBLEM STATEMENT	3
1.3 OBJECTIVES OF RESEARCH	3
1.4 SCOPE OF STUDY	4
CHAPTER 2 LITERATURE REVIEW	5
2.1 INTRODUCTION	5
2.2 X-RAY DIFFRACTION (XRD)	6
2.3 MICROSTRUCTURE OF CCTO AND CCTFO	8
2.4 DIELECTRIC PROPERTIES OF CCTO AND CCTFO	10

CHAPTER 3	MATERIALS AND METHODS	12
3.1	INTRODUCTION	12
3.2	MATERIAL SYNTHESIS METHODS	12
3.2.1	CALCULATION	13
3.2.2	GRINDING PROCEDURE	14
3.2.3	CALCINING AND DRYING	15
3.2.4	BINDER ADDITION	15
3.2.5	PELLETING	15
3.2.6	SINTERING	16
3.3	MATERIAL CHARACTERIZATIONS	16
3.3.1	X-RAY DIFFRACTION (XRD) CHARACTERIZATIONS	16
3.3.1.1	Principles of X-Ray Diffraction	16
3.3.1.2	X-Ray Diffraction Analysis Procedure	17
3.3.2	DIELECTRIC CHARACTERIZATION	18
3.3.2.1	Principles of Potentiostat	18
3.3.2.2	Dielectric Analysis Procedure	19
3.3.3	FIELD EMISSION SCANNING ELECTRON MICROSCOPY (FESEM)	19
3.3.3.1	Principles of FESEM	19
3.3.3.2	FESEM analysis	20
3.4	FLOW CHART	21
CHAPTER 4	RESULT AND DISCUSSION	22
4.1	X-RAY DIFFRACTION (XRD) ANALYSIS	22
4.2	FIELD EMISSION SCANNING ELECTRON MICROSCOPY (FESEM)	24
4.3	DIELECTRIC ANALYSIS	26
4.3.1	Dielectric Permittivity (ϵ')	26
4.3.2	Dielectric Loss ($\tan\delta$)	27

CHAPTER 5 CONCLUSION AND RECOMMENDATION	229
5.1 CONCLUSION	229
5.2 RECOMMENDATIONS	30
REFERENCE	31
APPENDICES.....	33
APPENDIX A.....	36
APPENDIX B.....	37
APPENDIX C.....	38
APPENDIX D.....	39
APPENDIX E.....	40
APPENDIX F.....	41

LIST OF TABLES

Table 2.1: Lattice parameter of pure and doped CCTO.....	6
Table 2.2: Grain size of CCTFO.....	7
Table 2.3: Grain size of CCTO.....	9
Table 2.4: The resistivity in grain (ρ_g) and resistivity in grain boundary (ρ_{gb}) fitted from the impedance spectra.....	10
Table 2.5: The Grains and grain boundaries resistance and capacitance of CCFTO ceramics.....	11
Table 3.1: Preparation of 10 g pure (undoped) CCTO sample.....	13
Table 3.2: Preparation of 10 g doped CCTO with Iron.(Fe) sample.....	13
Table 3.3: Preparation of 10 g doped CCTO with (Fe) sample.....	14
Table 4.1: The value of lattice parameter (a) in cubic structures of Iron doped CCTO with $x = 0, 0.05$ and 0.1	23
Table 4.2: Grain size of $x = 0, 0.05$ and 0.1 in $1\mu\text{m}$ at $\times 10\ 000$ Magnification.....	25
Table 4.3: Dielectric Permittivity of $x = 0, 0.05$ and 0.1	26
Table 4.4: Dielectric Loss ($\tan\delta$) of $x = 0, 0.005$ and 0.1	28

LIST OF FIGURES

Figure 1.1: Structure of $\text{CaCu}_3\text{Ti}_4\text{O}_{12}$ which shown octahedral of TiO_6 , Cu atoms bonded to four oxygen atoms, and Ca atom without bond.....	2
Figure 2.1: X-ray powder diffraction patterns of (a) CCTFO and (b) CCFTO respectively sintered at $900\text{ }^\circ\text{C}$ for 8 h.....	7
Figure 2.2: SEM micrograph of CCTFO sintered at $900\text{ }^\circ\text{C}$	8
Figure 3.1: Components of working principles of X-ray Diffraction.....	17
Figure 3.2: Bragg's Law of X-ray Diffraction.....	17
Figure 3.3: Working Principle of Potentiostat.....	18
Figure 3.4: Principle of FESEM operations.....	20
Figure 4.1: XRD pattern of Iron doped CCTO with $x = 0, 0.05$ and 0.1 at room temperature.....	22
Figure 4.2: Morphology of CCTO and CCTFO under FESEM at $\times 10\ 000$ Magnifications.....	25
Figure 4.4: Frequency dependence of dielectric loss ($\tan\delta$) of pure CCTO and doped CCTO with iron $x = 0, 0.05$ and 0.1	27

LIST OF SYMBOLS

ϵ'	-	Dielectric permittivity
$\tan(\delta)$	-	Dielectric loss
λ	-	Wavelength
μ	-	micron (10^{-6})
ϵ	-	Dielectric constant
2θ	-	Bragg angle
$^{\circ}\text{C}$	-	Degree Celcius
\AA	-	Angstrom (10^{-10})
ω	-	Angular velocity
g/mol	-	Molecular weight
A	-	Sample area
t	-	Sample thickness
ϵ_0	-	Permittivity of free space
a	-	Lattice parameter
Z_i	-	Imaginary impedance
Z_r	-	Real impedance

LIST OF ABBREVIATIONS

CCTO	-	Calcium copper titanium oxide
CCTFO	-	Calcium copper titanium iron oxide
Ca	-	Calcium
Cu	-	Copper
Ti	-	Titanium
Fe	-	Iron
O	-	Oxygen
IBLC	-	Internal barrier layer capacitance
EDLC	-	electrochemical double layer capacitance
FESEM	-	Field Emission Scanning Electron Microscopic
XRD	-	X-ray diffraction
PVA	-	Polyvinyl alcohol
Y	-	Ytterium

CHAPTER 1

INTRODUCTION

1.1 BACKGROUND OF STUDY

Microelectronic can be defined as the area of technology that associated with and applied to realization of electronic systems which is extremely small electronic elements or parts. Basically, microelectronic is subfield of electronic devices, which are relates to the manufacture and study of components and electronic designs. Few years ago, the discovery of high permittivity in Calcium Copper Titanate (CCTO) by Subramanian *et al.*, (2000), CCTO has become an important and suitable ceramic material to replace commonly used high-dielectric materials. CCTO had high dielectric constant which is more than 10^4 , and also has a good stability, beside, it also has low loss tangent. CCTO structure is a complex body centered cubic perovskite oxide having a very large value of dielectric and almost constant in temperature range 100-600 K. The structure of CCTO was derived from the cubic perovskite (ABO_3) by an octahedral tilt distortion which caused by mismatch of the size and the nature of A cations. Meanwhile, the TiO_6 octahedral tilt produce a structure where three quarter of the A sites have quarter planar coordination which are occupied with Cu ions and the remaining quarters of the sites are occupied by Ca atom which is have 12 fold coordination.

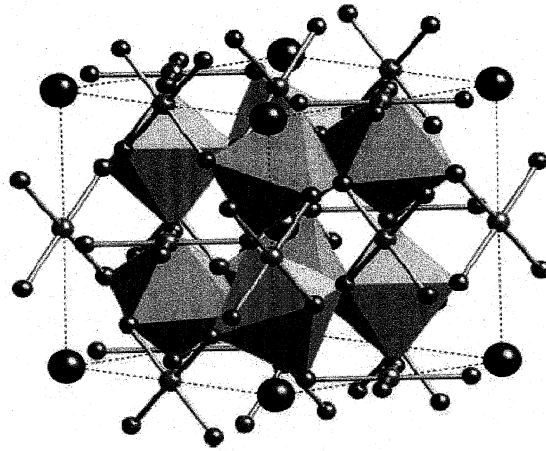


Figure 1.1: Structure of $\text{CaCu}_3\text{Ti}_4\text{O}_{12}$ which shown octahedral of TiO_6 , Cu atoms bonded to four oxygen atoms, and Ca atom without bond.

Source: Sunil Patra *et al.*, 2009

Mostly, materials with high dielectric constants are widely used in many applications in technology such as supercapacitor, capacitor, resonators and filters. Because of the high dielectric constant, CCTO is allowed smaller capacitive components, which are offering the opportunity to decrease the size of the electronic devices. With the ability to reduce the size of the electronic device, CCTO become the most important material in production of electronic devices.

Unfortunately, the origin of this giant high dielectric constant (high permittivity) are still unknown and not clear and intensively discussed in literature. However, a researcher like Homes *et al.*, and Ramirez *et al.*, explained the temperature behavior of permittivity in CCTO single crystals. They suggest that the polarization of mechanism involving displacement of Ti^{4+} ions from the center of symmetry within the octahedral sites. However, until today there is no experimental and research evidence to support this theory. Meanwhile, Li *et al.* and Whangbo and Subramanian, argued that the factor that caused high permittivity in CCTO was the present of intrinsic twin boundaries or planar defects. But nowadays, most of researcher accept the theory that the association of internal barrier layer capacitance (IBLC) with present of high dielectric constant of CCTO. Even though CCTO has high dielectric constant, but it also has high dielectric loss.

1.2 PROBLEM STATEMENT

Over the year, high dielectric constant are found in ferroelectric materials, but unfortunately calcium copper titanate (CCTO) is not a ferroelectric material and therefore, further studies about CCTO ceramics is ongoing. Most of the researchers are still had argument about the origin of high dielectric constant in CCTO ceramics. However, recently studied was found out that even though CCTO has high dielectric constant, it also had high dielectric loss. Fabrication of CCTO with certain element such as Yb, La and Fe will alter the dielectric properties and morphology of the CCTO. In this experiment, CCTO will doped with Fe^{3+} in order to understand and learn the factor that cause high dielectric loss in CCTO.

1.3 OBJECTIVES OF RESEARCH

Objectives of this research are:

1. To synthesis calcium copper titanate (CCTO) doped with Fe^{3+} with composition of $x = 0.00$, $x = 0.05$ and $x = 0.1$ through solid state method.
2. To study the dielectric loss and dielectric permittivity of calcium copper titanate (CCTO) doped with Fe^{3+} using Potentiostat.
3. To investigate the morphology of calcium copper titanate (CCTO) doped with Fe^{3+} via FESEM.

1.4 SCOPE OF STUDY

In this experiment calcium copper titanate (CCTO) will be doped with iron by using solid-state method. Before the doping process, all the material should be well prepared. The high purity of CaCO_3 (99.99 %), CuO (99.99 %), TiO_2 (99.99 %), and Fe_2O_3 (99.99 %) is required and there should be no contamination on the materials. The amount (in gram) of each material that will use in the experiment was calculated. Then the amount of x (Fe content) was fixed to 0.00, 0.05, and 0.1. According to the objective of my experiment, the amount of x will determine the dielectric loss of calcium copper titanate iron (CCTFO) ceramic. After all the materials are well prepared, the solid-state method will be carried out. To characterize the crystalline structure of the CCTFO, the X-ray diffraction (XRD) (D/max-2550/PC, Rigaku, Japan) method will be used with Cu K-alpha radiation. Meanwhile, the microstructure of the CCTFO ceramics will be studied by Field Emission Scanning Electron Microscope (FESEM). Then the Potentiostat instrument will be used to study the electrical properties of CCTFO.

CHAPTER 2

LITERATURE REVIEW

2.1 INTRODUCTION

Lately, calcium copper titanate (CCTO) ceramics have attract considerable interests in many application of technology. This is because of the CCTO ceramics has high dielectric constant. The developments of microelectronics devices encourage people to search a new ceramic material that can performance in devices with high dielectric permittivity, also whose performance in device such as capacitors which not compromised as the size of the components becomes smaller. The accepted mechanism that used to explain a giant dielectric constant in CCTO is the formation of internal barriers layer (IBL) due to the inhomogeneous microstructure consisting of semiconducting grains and insulating grains boundaries.

Generally, the preparation of CCTO can be done using conventional solid-state method, but this method caused inhomogeneity and other limitation of the CCTO. It is well know that when the ceramic is a homogenous microstructure the properties of dielectric can be considerably improved. But, some researchers used other method to dope CCTO such as sol-gel method. This method has an advantage of preparing multi component system with high homogeneity, because the mixing process is carried out at the molecular level. Compared with solid-state method (conventional mechanical milling method) for the preparation of raw powder, the sol-gel method are able to obtain the homogenous raw powder in size of nano-meter to encourage a fine microstructure of the sintered ceramic.

2.2 X-RAY DIFFRACTION (XRD)

K.D Mandal *et al*, method to determine the lattice parameter and unit cell volume. The theoretical value of lattice parameter of pure CCTO is 7.391 Å. Theoretically, CCTO is a complex body centered cubic perovskite oxide structure. Beside, from table 2.2 conclude that changing Fe doping site does not change the cubic perovskite structure. But however, the changing Fe doping site can cause the increasing of unit cell volume of CCTFO. For example when the dopant site at Ti⁴⁺, the lattice parameter is 7.382±0.152 Å, meanwhile, when the dopant site change at Cu, the lattice parameter is 7.379 ± 0.216 Å, which both value are almost similar with slightly highest compare to pure CCTO lattice parameter (K.D Mandal et al, 2014).

Table 2.1: Lattice parameter of pure and doped CCTO.

Sample	Lattice parameter (Å)
CCTO	7.391
CCTFO	7.382±0.152
CCFTO	7.379 ± 0.216

Source: K.D Mandal et al, 2014

Meanwhile, changing the Fe doping site does not affect the XRD pattern of CCTO. From Figure 2.1, it shows that the XRD patterns of CCTFO and CCFTO are in good agreement with un-doped CCTO. From this result, they confirm that pure CCTO has formation of major phase of CCTO. Meanwhile doped CCTO has formation of minor phase of CCTO. As expected result, pure CCTO powder is only can be obtained when the ratio of calcium, copper and titanium are very close to stoichiometric (A. Loidl et al). The curves of sample CCTFO and CCFTO were almost identical with pure CCTO, which indicate that the doping process of CCTO does not influence the crystalline nature of CCTO ceramic.

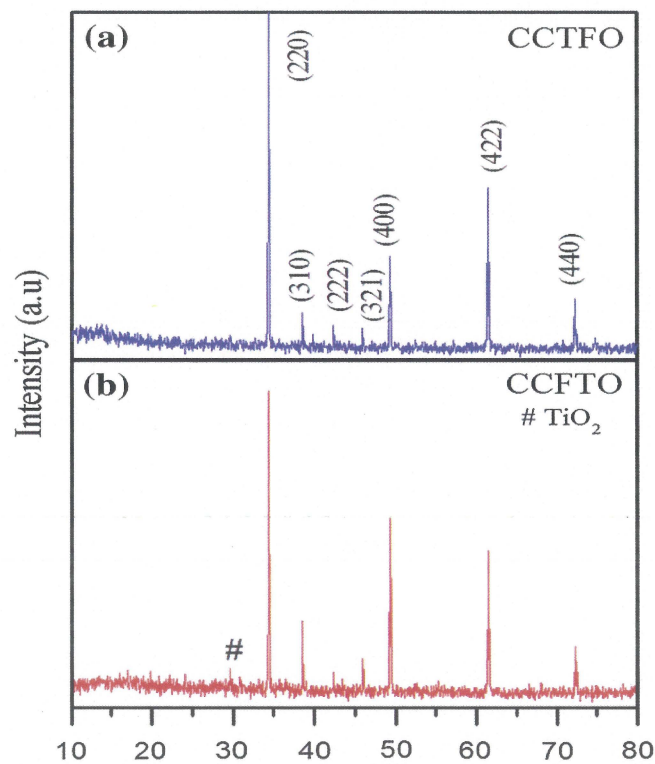


Figure 2.1: X-ray powder diffraction patterns of (a) CCTFO and (b) CCFTO respectively sintered at 900 °C for 8 h.

Source: K.D Mandal et al., 2014

2.3 MICROSTRUCTURE OF CCTO AND CCTFO

From Figure 2.2, the microstructure of the sample shows the presence of precipitate at grainboundaries. It can be that the existing of precipitated at grainboundaries was caused by the formation of liquid phase during sintering process. Other than that, from their analysis, they manage to observed a 9-10 μm of grain size of the microstructure, which is smaller than that reported earlier (K.D Mandal et al., 2014). The grain size according to Table 2.2 was 9-10 μm are observed in the microstructure of doped CCTFO. This grain size value is less than they report earlier. This is because lower temperature was used which is 900 $^{\circ}\text{C}$ compare the previous experiments (Singh N.K et al, 2001)

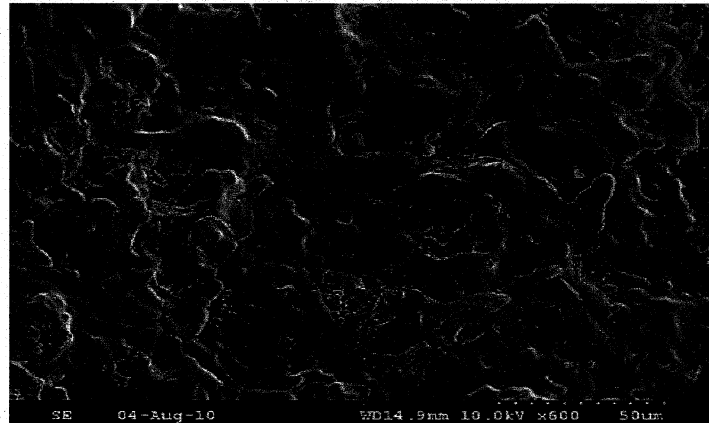


Figure 2.2: SEM micrograph of CCTFO sintered at 900 $^{\circ}\text{C}$
Source: Alok Kumar et al., 2011

Table 2.2: Grain size of CCTFO

Sample	Grain size
CCTFO	9-10 μm

Source: Sang K.L et al, 2011

From the table, when the amount of Fe doping content increase, the average grain size also will increase. At pure CCTO, it shows the discontinuous grain growth. Meanwhile at the composition of $x = 0.01$ and $x = 0.04$, the grain growth could be seen clearly and the average grain size increase until $50 \mu\text{m}$ and $100 \mu\text{m}$ respectively. If the amount of Fe is $x = 0.2$, the average grain size could be increased up to $120 \mu\text{m}$. This situation due to the charge is compensated by formation of cation vacancies, which interact with oxygen vacancies and decrease their mobility. As oxygen vacancies play an important role in structure mobility, we observe smaller crystalline size and also particle size. In case of acceptor doping the situation is opposite, oxygen vacancies form, and we obtain larger crystals than without doping.

Table 2.3: Grain size of doped CCTO

Sample	Grain size
$x = 0.01$	$50 \mu\text{m}$
$x = 0.04$	$100 \mu\text{m}$
$x = 0.2$	$120 \mu\text{m}$

Source: Laxman Singh et al., (2007)

2.4 DIELECTRIC PROPERTIES OF CCTO AND CCTFO

Table 2.4 shows that if the sample is un-doped (pure sample of CCTO), the grain resistivity is lower than grain boundaries resistivity. Meanwhile, in doped sample, when the composition of iron x is increases, the resistivity of both grain and grain boundaries are also increases.

According to the experiment that has done by Alok Kumar et al, in room temperature, when the amount of iron (Fe^{3+}) increased, the dielectric constant (ϵ') of CCTFO will decrease. Meanwhile, at high temperature (above room temperature), the dielectric constant (ϵ') are re-increased at high level. Table 2.5 shows that grains as well as grain boundaries are insulating. This suppresses the formation of barrier layers explaining the low value of dielectric constant (ϵ') of the CCTFO ceramics.

From the Table 2.5 shows that the grain resistance is decreasing when the temperature is increased. They also conclude that, the grain boundaries resistance will decrease when the temperature increased, but at temperature 350 K there is no value of grain boundaries resistance. Same goes with grain capacitance and grain boundaries capacitance, which it will decrease when the temperature is increased.

Table 2.4: The resistivity in grain (ρ_g) and resistivity in grain boundary (ρ_{gb}) fitted from the impedance spectra.

Composition of x	Resistivity in grain (ρ_g)	Resistivity in grain boundaries (ρ_{gb})
0	4.65×10^{-10}	1.30×10^4
0.015	4.26	-
0.03	4.82×10^3	1.68×10^4
0.0045	1.46×10^4	2.86×10^4
0.06	1.91×10^4	4.08×10^4

Source: Zhi Yang et al., (2012)

Table 2.5: Grains and grain boundaries resistance and capacitance of CCFTO ceramics.

Temperature (K)	R_g (Ohm)	R_{gb} (Ohm)	C_g (F)	C_{gb} (F)
350	1.93×10^6	-	3.99×10^{-11}	-
400	2.40×10^5	6.70×10^5	4.26×10^{-11}	2.38×10^{-9}
450	3.43×10^4	8.49×10^4	3.96×10^{-11}	4.98×10^{-9}

Source: Alok Kumar et al. (2011)

CHAPTER 3

MATERIALS AND METHODS

3.1 INTRODUCTION

In this chapter, the research methodology will explain more details step by step. There are two stages that involve in this research which are first is materials synthesis method, and second is material characterization method. In first stage which is materials synthesis, there are seven steps involved which are calculation, grinding, calcination, binder addition, pelleting and sintering, which are later will be explain in more details. For the second stage which is material characterization, there are three steps involved which are X-ray diffraction (XRD) characterization, dielectric characterization and Field Emission Scanning Electron Microscopy (FESEM).

3.2 MATERIAL SYNTHESIS METHODS

The stoichiometric undoped samples of CCTO sample was doped with cations Fe^{3+} substituting Ti^{4+} cations. The sample (CCTO and CCTFO) was synthesized by using conventional Solid State Reaction route. This method is the most widely used in preparation of polycrystalline solids which is from mixture of solid starting materials. Basically solid does not react together at room temperature, so approximately 900 °C to 1500 °C temperature is required for the reaction occur. More details will be explained in this stage.

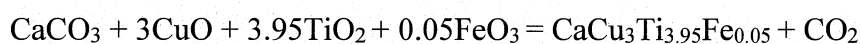
3.2.1 CALCULATIONS

There are three (3) type of sample used in this experiment which is pure CCTO, doped CCTO with Fe^{3+} amount of $x = 0.05$ and $x = 0.1$. The mass of each sample is 10 g.

As for a starting powders which is pure sample:



Doped sample at Ti site with Fe^{3+} which the value of $x = 0.05$ g:



Doped sample at Ti site with Fe^{3+} which the value of $x = 0.1$ g:

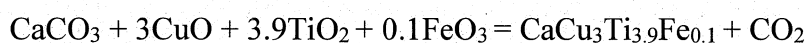


Table 3.1: Preparation of 10 g pure (undoped) CCTO sample

Type of powder used	Molecular weight g/mol	Mass gram (g)
CaCO_3	100.07	1.52
3CuO	238.63	3.63
4TiO ₂	319.46	4.85
Total	658.1767	10

Table 3.2: preparation of 10 g doped CCTO with Iron (Fe) $x = 0.05$ sample.

Type of powder used	Molecular weight g/mol	Mass gram (g)
CaCO_3	100.07	1.47
3CuO	238.638	3.50
3.95TiO ₂	315.47	4.63
0.05FeO ₃	26.79	0.39
Total	680.97	10

Table 3.3: Preparation of 10 g doped CCTO with (Fe) $x = 0.1$ sample.

Type of powder used	Molecular weight g/mol	Mass gram (g)
CaCO ₃	100.07	1.46
3CuO	238.63	3.50
3.9TiO ₂	311.48	4.58
0.1FeO ₃	29.58	0.43
	Total: 679.783	Total: 10

3.2.2 GRINDING PROCEDURE

The raw materials then mixed thoroughly inside the mortar pestle then grinded slowly by using hand for 10 hours. Ethanol was used as a grinding medium. A medium size of mortar pestle was used to grind the CCTO and CCTFO powder. The steps of grinding the powder as shown below:

Step 1: The mortar pestle was cleaned by using ethanol solution and then dried for few minutes before used.

Step 2: The sample was poured into mortar pestle slowly and gently. Then the grinding process was started and the stopwatch also started at the same time.

Step 3: A few ethanol solutions poured into CCTO or CCTFO powder while grinding the powder. The purpose of the ethanol solution is to make sure the powder will mix well and even.

Step 4: After 10 hours, which is the grinding process is complete, the powder was removed and the mortar pestle was cleaned by using ethanol and detergent.

3.2.3 CALCINING AND DRYING

Calcination is the process where the synthesized powder will be exposed to heat at high temperature in air or oxygen. The purpose of calcination process is to driven out the sample powder moisture, volatile impurities of S, As and P as their volatile oxides. For this experiment, the calcination process was carried out in air where the temperature used is 900 °C. The furnace heating rate is about 5 to 10 °C per minute. The furnace approximately took 3 to 4 hours to reach the desired temperature which is 900 °C. Then the furnace was cooled for 12 hours before took the sample from inside the furnace. Basically, the calcination process is affected by the mechanical and electrical properties of the ceramics to large extent. At high calcination temperature, the density and homogeneity of the resultant ceramic will be high as well so, the calcination process should be taken more carefully.

3.2.4 BINDER ADDITION

The calcined powder of CCTO and CCTFO at 900 °C then mixed with polyvinyl alcohol (PVA) which is PVA acts as a binder. The purpose of adding binder is, the binder can helps in increasing the mechanical strength of the pellets so that the pellets can be used for sintering process.

3.2.5 PELLETING

After the addition of PVA binder into CCTO and CCTFO powder, the sample powder was converted to cylindrical shaped pellet by using hydraulic pressure instrument. Each pellet has 0.5 g of thickness which are these method of pressing of powder includes die pressing. The technique of pressing pellet was using 3 to 4 ton of pressure and not more than 10 seconds hold. To avoid the crack of pellet from happen, the pressure ton should be reduce from 4 to 3 ton pressure of the hydraulic pressure. Other than that, the pellet cracking can be avoided by carried out the pelleting process more gently and slowly.

3.2.6 SINTERING

The complete pellets then sintered in conventional furnace of temperature at 1000 °C in air for 8 hours. The heating rate of furnace is about 5 to 10 °C per minute and will reach the desired temperature approximately 4 hours. During the sintering stage, the pellets were heated so it can produce the desired microstructure.

3.3 MATERIAL CHARACTERIZATIONS

There are three steps involved in this stage which are XRD, dielectric and FESEM characterizations. Before the materials characterization started, Potentiostat and FESEM sample was coated by proper coating material. For Potentiostat characterization, the pellet was coated using silver paste. Meanwhile for FESEM characterization, the pellet was coated using platinum.

3.3.1 X-RAY DIFFRACTION (XRD) CHARACTERIZATIONS

3.3.1.1 Principles of X-ray Diffraction

X-ray diffraction (XRD) is a non-destructive technique that widely used in industry. Basically X-ray diffraction is depends on the interference of crystalline and monochromatic X-rays sample. The purpose of X-ray diffraction is to determine the arrangement of atoms within crystal including crystalline size and its orientation, chain orientation and phase analysis. The arrangement of X-ray components as shown in Figure 3.1.

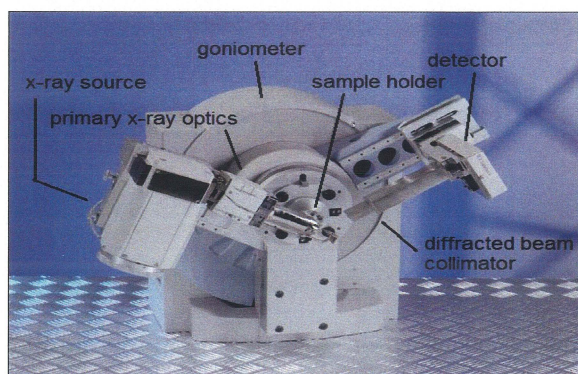


Figure 3.1: Components of working principles of X-ray Diffraction

X-ray Diffraction obeys Bragg's Law. The interaction of the incident rays of the sample will produce constructive interference if the condition is satisfied by Bragg's Law. The Bragg's Law conditions are shown in Figure 3.2.

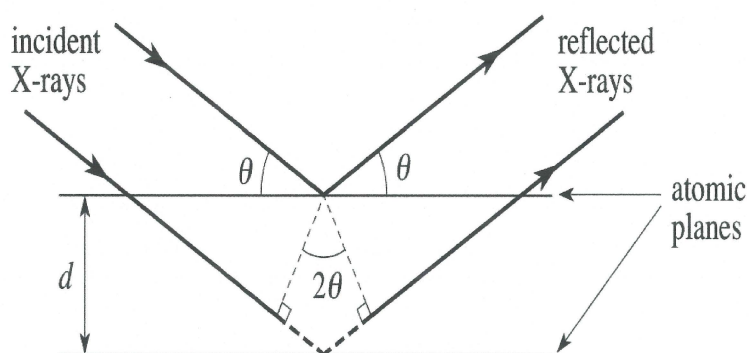


Figure 3.2: Bragg's Law of X-ray Diffraction

3.3.1.2 X-ray Diffraction Analysis Procedure

The calcined powder was taken into X-ray Diffraction and ready for XRD analysis. The sample was poured into glass holder then, the glass holder that contains calcined powder was inserted into XRD machine sample holder. The elements that were analyzed are $\text{CaCu}_3\text{Ti}_4\text{Fe O}_{12}$. The analysis was run at $2\theta = 20^\circ$ to 80° at a rate of $1^\circ/\text{min}$ with $\text{Cu K}\alpha$ ($\lambda = 1.5406 \text{ \AA}$) radiation.

3.3.2 DIELECTRIC CHARACTERIZATION BY USING POTENTIOSTAT

3.3.2.1 Principle of Potentiostat

Potentiostat is an electronic instrument that controls and measures the voltage difference between reference electrode and a working electrode. Potentiostat also measure the current flow between counter electrodes and working electrode. Basically there are three electrodes involved in Potentiostat analysis which are working electrode, reference electrode and counter electrode.

The role of working electrode is as a sample of the corroding metal that being tested. Reference electrode is as an electrode with a constant electrochemical potential and counter electrode as a current-carrying electrode that completes the cell circuit. The reason of Potentiostat have three electrodes is because it will allows the potential at the working electrode and the current at the working electrode can be measured with no interference or little contribution from other electrodes. The diagram of working principle of Potentiostat is shown in figure 3.3.

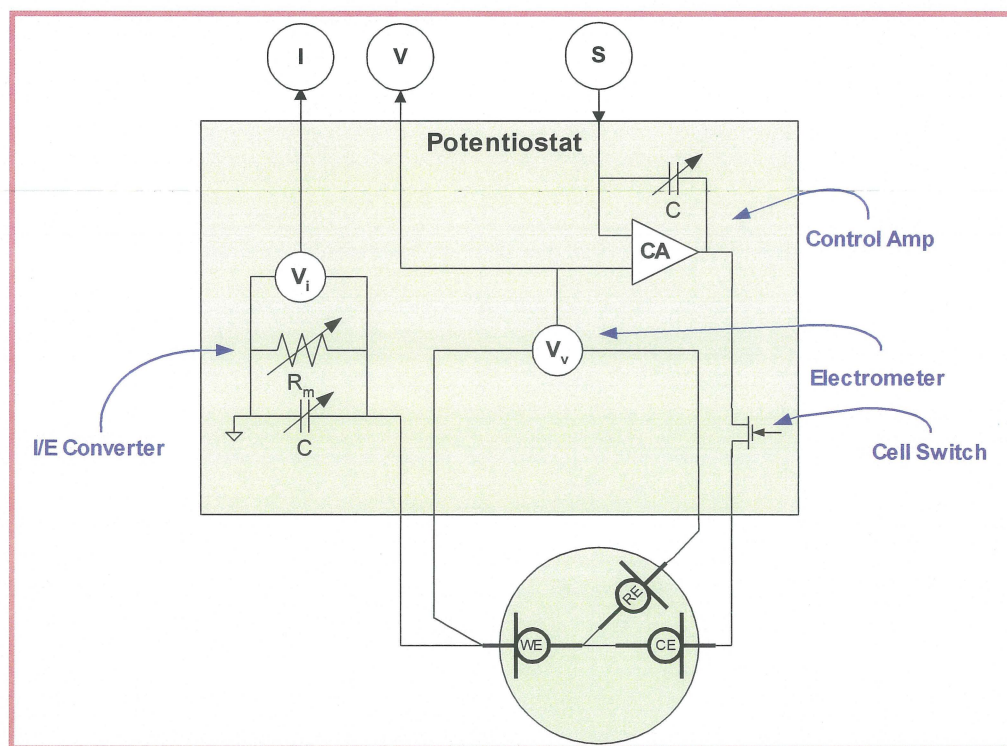


Figure 3.3: Working principle of Potentiostat

3.3.2.2 Dielectric Analysis Procedure

The calcined powder was taken into Potentiostat laboratory for the analysis process. Before the analysis process started, the sample (pellet) was coated with silver paste dried for a few minutes. Then the pellet was inserted into sample holder and the analysis process was begun.

3.3.3 FIELD EMISSION SCANNING ELECTRON MICROSCOPY (FESEM)

3.3.3.1 Principle of FESEM

FESEM is a microscope that works together with electrons which are particles with negative charge instead of using light. These electrons are liberated by a field emission source, and the sample is scanned by electrons according to a zigzag pattern. The purpose of invention FESEM is to visualize nanostructures of samples surface. The working principle of FESEM start when the electrons are liberated from a field emission source of and it accelerated in high electrical field gradient. Then, inside the high vacuum column so-called primary electrons are deflected and focused by electronic lenses which will produce a narrow scan beam that bombards the sample/object. Then, the next process is the secondary electrons are emitted from each spot on the sample/object. After that, a detector are catches the secondary electrons and produces an electronic signal. Finally, this electronic signal is transformed and amplified to a video scan-image which that can be seen on a monitor. The diagram of working principle of FESEM shows as Figure 3.4.

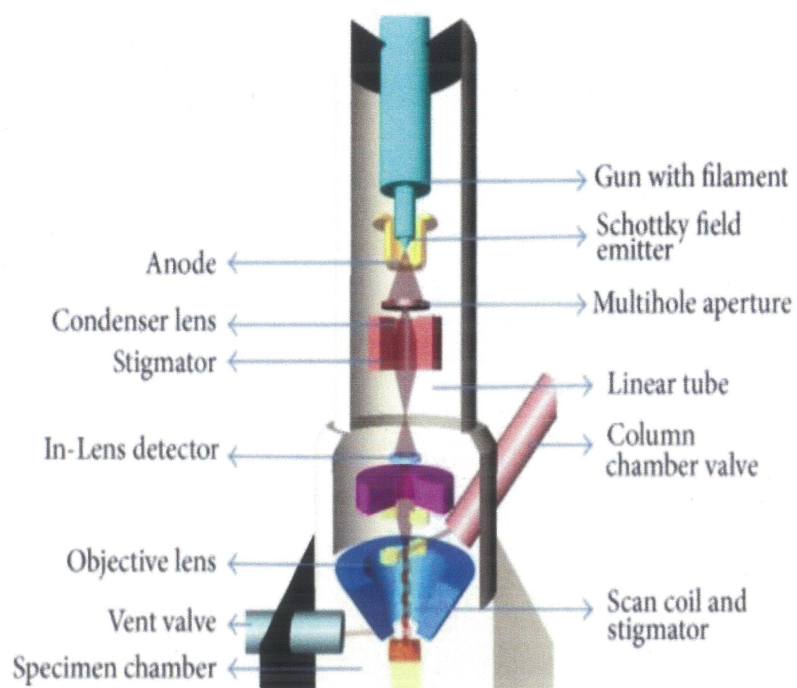


Figure 3.4: Principle of FESEM operations

3.3.3.2 FESEM Analysis

The calcined sample (pellet) was mounted on an aluminum stub and then attached using sticky conducting tape. Then, a layer of around 0.5 cm was coated by using platinum on top of the sample holder. The microstructure or morphology of the sample was analyzed using FESEM.

CHAPTER 4

RESULT AND DISCUSSION

4.1 X-RAY DIFFRACTION (XRD) ANALYSIS

Figure 4.1 shows the XRD patterns of pure CCTO and doped CCTFO with $x = 0.05$ and 0.1 , which are calcined at $1000\text{ }^{\circ}\text{C}$ for 8 hours. At the composition we get sharp peaks in the 2θ range at 29.66° , 31.30° , 38.55° , 49.338° , 61.44° and 72.27° which were found to have a good matching with theoretical value of CCTO. The graph pattern slightly shifted as the angle increase when pure CCTO dope with iron. At peak (211) and (220) are shows a slight shift indicates the changing of crystal plane when the sample is doped with iron. The doping of iron (Fe) does not have a huge influence to the nature of CCTO. From XRD data, there are no significant of secondary phase that could be detected in the XRD data. This is due probably due to the quantities or amount of iron (Fe^{3+}) doped with CCTO may lower than the detection limits of the technique.

The value of lattice parameter of each samples were calculated at same peak of each phase as shown as Table 4.1. As the x contents increase the lattice parameter of the sample will decrease. This decrease of the lattice parameter is with doping contents may due to the difference in ionic radius of dopant Fe^{3+} (0.785\AA) to that of parent Ti^{4+} (0.745\AA) ion.

Figure 4.1: XRD pattern of Iron doped CCTO with $x = 0, 0.05$ and 0.1 at room temperature.

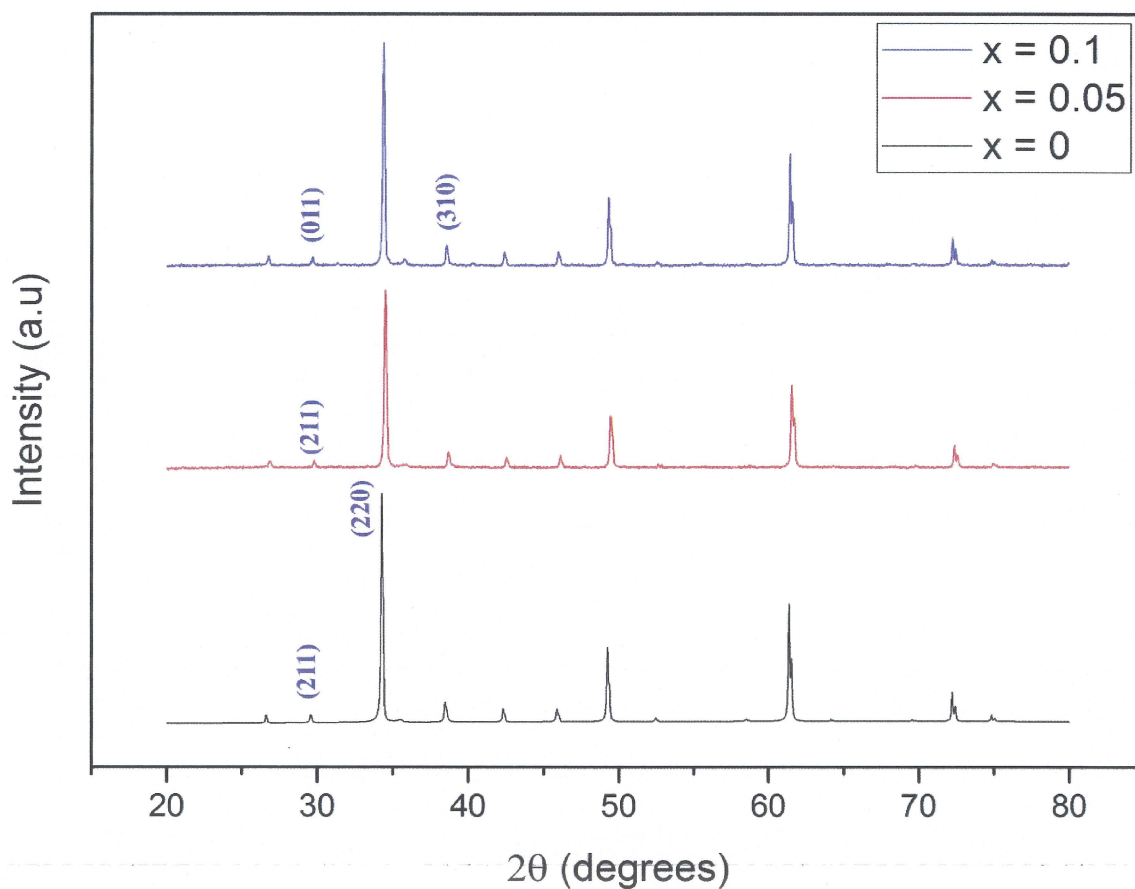


Table 4.1: The value of lattice parameter (a) in cubic structures of Iron doped CCTO with $x = 0, 0.05$ and 0.1

Sample	Phase	Lattice Parameter (\AA)
$x = 0$	(211)	8.3837
$x = 0.05$	(211)	7.3145
$x = 0.1$	(011)	4.2600

4.2 FIELD EMISSION SCANNING ELECTRON MICROSCOPY (FESEM) ANALYSIS

The morphology of pure CCTO and doped CCTFO were studied by using FESEM. Each sample was analyzed in with different magnification to get a comparison between each sample and the size of each image is 1 μm . The FESEM images of the CCTO and CCTFO ceramics which sintered at 1000 $^{\circ}\text{C}$ for 10 hours was presented as below.

Figure 4.2 (a) shows the microstructure of pure sample of CCTO. Microstructure of the pure sample CCTO shows the presence of precipitate at grainboundaries. The presence of precipitate may occur due to a liquid phase that formed during sintering process, which could assist the densification of the ceramics materials. Microstructure of CCTO shows matrix of consisting of large grains where small grains are embedded in betweenlarger grains. The average size of grains growth are very small which is 161 μm .

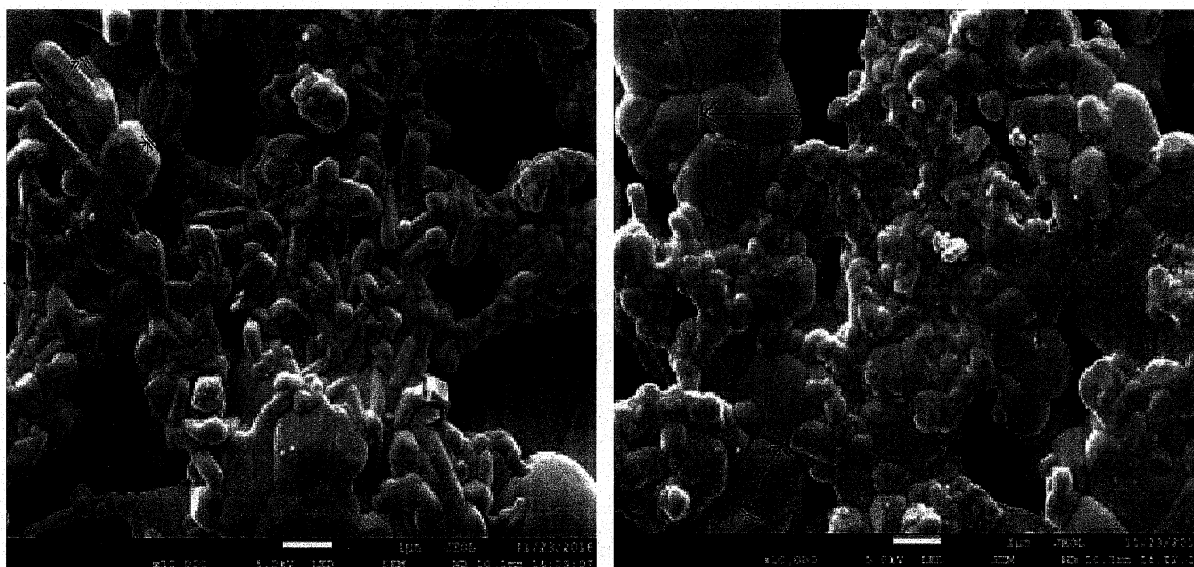
Other than that, there are porosity that can be observed on pure CCTO image. The porosity that present in the samples are intragranular in nature.

Figure 4.2 (b) shows the microstructure of doped CCTFO, $x = 0.05$. The microsturcture of this sample also shows some traces of precipitates at grain boundaries. The average grains size of this sample is larger compare to pure CCTO which is 169 μm . Meanwhile, the pores that exist in this sample are smaller compare to pure sample.

Figure (c) shows the microstructure of CCTFO $x = 0.1$. There are presences of precipitates at grain boundaries, which are due to existence of liquid phases formed during sintering process. The average grains size of this sample is larger which is 231 μm compare to pure and CCTFO $x = 0.05$ samples. On the other hand, the sizes of pores of this sample are getting smaller compares the others two sample.

Table 4.2: Grain size of $x = 0, 0.05$ and 0.1 in $1\mu\text{m}$ at $\times 10\ 000$ magnification

Sample	Average grain size measured in μm
$x = 0$	161
$x = 0.05$	169
$x = 0.1$	231



(a)

(b)



(c)

Figure 4.2: Morphology of CCTO and CCTFO under FESEM at $\times 10\ 000$ magnifications.

4.3 DIELECTRIC ANALYSIS

4.3.1 Dielectric Permittivity (ϵ') of $x = 0, 0.05$ and 0.1

Figure 4.3 shows the frequency dependence of dielectric permittivity (ϵ') of pure CCTO and doped CCTFO sample with $x = 0.05$ and 0.1 . From the plotted graph above, pure CCTO ($x = 0$) exhibits highest value of dielectric properties which is 9382, but decreases rapidly at frequencies 12 Hz. Meanwhile, the dielectric permittivity of doped CCTO with iron shows a lower value compare to pure CCTO. For doped sample of CCTFO with $x = 0.05$, the dielectric permittivity is decrease dramatically from 9382 to 6731, but the frequencies are decrease slowly. Meanwhile, at $x = 0.1$ the value of dielectric permittivity of CCTFO are 8000 which it decrease rapidly over frequencies. So the changing trend of the dielectric permittivity in doped sample (CCTFO) ceramics is inconsistent with increasing x amount.

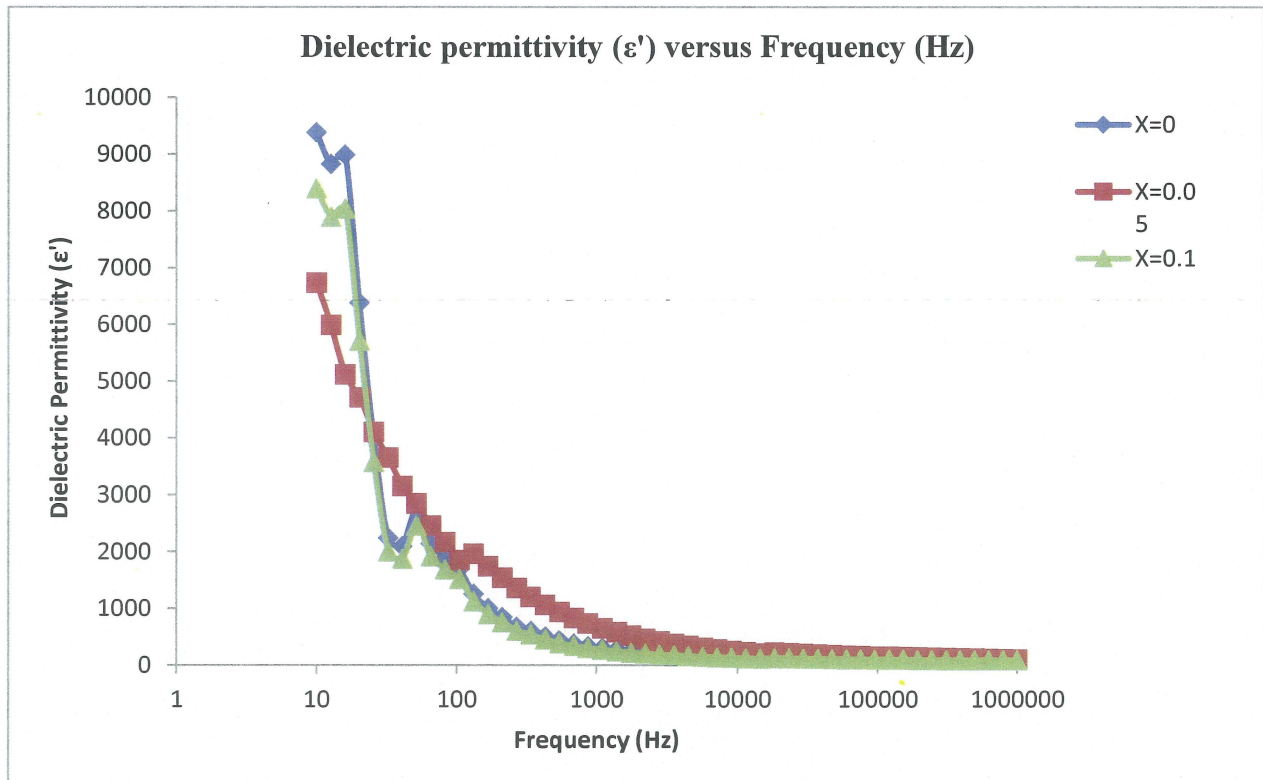


Figure 4.3: Frequency dependence of dielectric permittivity of pure CCTO and doped CCTO with iron $x = 0, 0.05$ and 0.1 .

Table 4.3: Dielectric Permittivity of $x = 0, 0.05$ and 0.1

Sample	Dielectric Permittivity
$x = 0$	9382
$x = 0.05$	6731
$x = 0.1$	8391

4.3.2 Dielectric Loss ($\tan\delta$) of $x=0, 0.05$ and 0.1

Figure 4.4 shows the frequency dependence of dielectric loss ($\tan\delta$) of pure CCTO and doped CCTFO sample with $x = 0.05$ and 0.1 . From the plotted graph above, pure CCTO ($x = 0$) exhibits highest value of dielectric loss which is 78588 and it decrease rapidly over frequencies. For doped sample with iron $x = 0.05$, shows the lowest value at frequency 10 Hz which is 52265 and it also decrease rapidly over frequencies. Meanwhile the value of dielectric loss ($\tan\delta$) of $x = 0.1$ at 10 Hz is 70666. So the changing trend of the dielectric loss ($\tan\delta$) in doped sample (CCTFO) ceramics is inconsistent with increasing x amount.

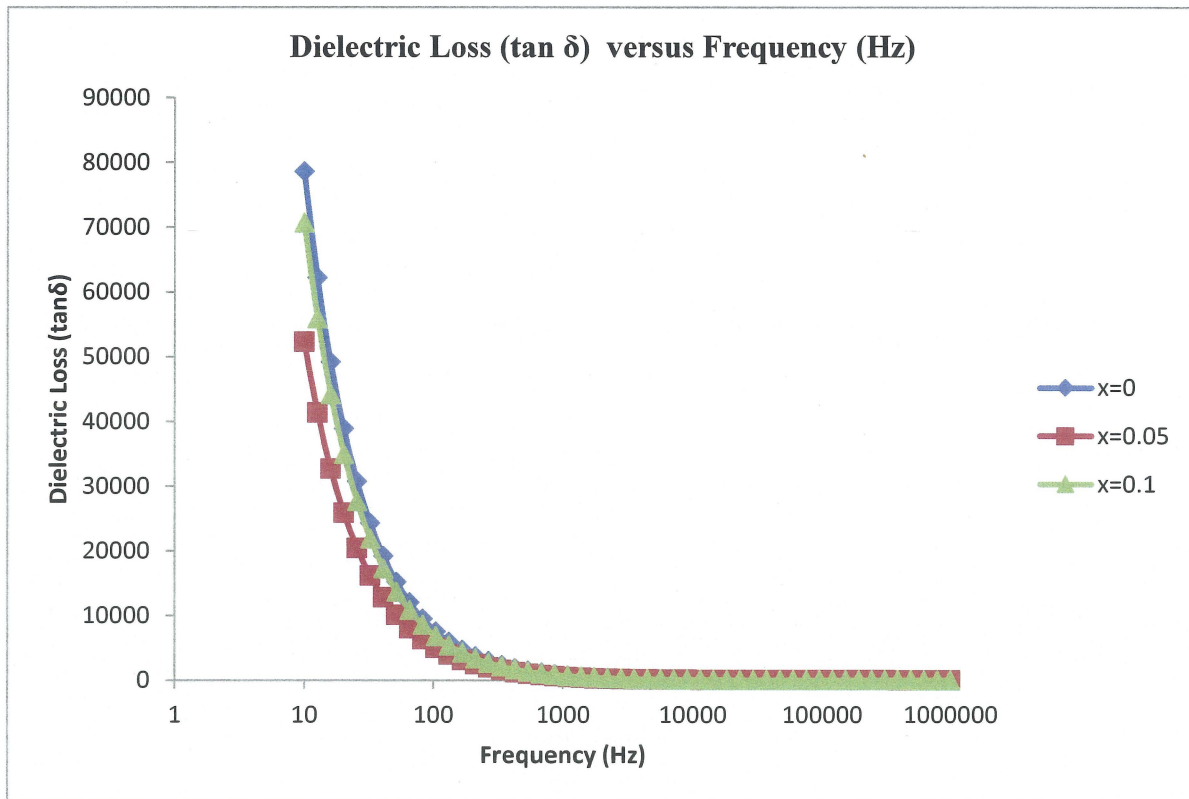


Figure 4.4: Frequency dependence of dielectric loss ($\tan\delta$) of pure CCTO and doped CCTO with iron $x = 0, 0.05$ and 0.1 .

Table 4.4: Dielectric Loss ($\tan\delta$) of $x = 0, 0.005$ and 0.1

Sample	Dielectric Loss ($\tan\delta$)
$x = 0$	78588
$x = 0.05$	52265
$x = 0.1$	70666

CHAPTER 5

CONCLUSION AND RECOMMENDATION

5.1 CONCLUSION

The pure CCTO and doped CCTFO are successfully synthesized by solid state reaction route. The preliminary objective of this project is to synthesis and analysis pure CCTO and doped CCTO with Iron (Fe^{3+}). The XRD peaks reveal the formation of single phase of cubic perovskite structure for the composition. The FESEM micrographs showed the dense microstructure for CCTO and CCTFO ceramics sintered at temperature 1000°C . The growth of average grain size for pure CCTO sintered at temperature 1000°C for 10 hours is lower as compared to that doped CCTFO. The dielectric permittivity of pure CCTO is the highest value at frequency 10 Hz. For doped sample $x = 0.05$ is the lowest dielectric permittivity value. Meanwhile for dielectric loss, a pure CCTO shows the highest value at frequency 10 Hz and for doped sample, $x = 0.05$ is the lowest dielectric loss and follow by $x = 0.1$. The doping process does not increase the dielectric properties of CCTO but it can alter the dielectric properties of CCTO for many applications.

5.2 RECOMMENDATIONS

There are some limitations in this project, therefore it is required to have some recommendation to improve the result of the project. One of the limitation is the grinding methods should done by using ball milled instrument, so that a very fine powder of CCTO and CCTFO can be produced. Other than that, the pelleting process should carried out more carefully to avoid a crack on pellets sample because the crack could interfered the dielectric properties results. Moreover, to get more accurate result in dielectric properties use the impedance analyzer instead potentiostat. Furthermore, higher temperature of furnace during calcined and sintered process should be used to obtain the optimum prepared sample.

REFERENCE

- Huiling Gong, X. (2014). Grain size effect on electrical and reliability characteristics of modified. *Journal of the European Ceramics Society*, 1733-1739.
- Supriya Chandra. Synthesis and Characterization of CCTO Ceramics by Solid State Reaction Route. *Department of Physics National Institute Of Technology Rourkela*, Roll-411PH2091.
- C. C. Homes, T. Vogt, S. M. Shapiro, S. Wakimoto, and A. P. Ramirez, (2001) *Science Appl. Phys. Lett.* **293**, 673.
- "Dielectrics-physics".*Britannica*.2009. p. 1. Retrieved 2009-08-12..
- W. Si, E. M. Cruz, P. D. Johnson, P. W. Barnes, P. Woodward, and A. P. Ramirez, (2002). *Appl. Phys. Lett* **81**, 2056.
- Julie J. Mohamed, Sabar D. Hutagalung , M. Fadzil Ain , Karim Deraman , Zainal A.Ahmad, (2002). *Materials Letters* **61** x1835–1838.
- M. A. Subramanian and A. W. Sleight, (2002). *Solid State Sci.* **4**, 347
- Alok K.R, N.K Singh. (2011). Dielectric Properties of Iron Calcium Copper Titanate, CaCu₃Ti_{3.9}Fe_{0.1}O₁₂ Ceramic. *science+business, LLC*.
- Hiroshi kishi, Y. M (2003). Base-Metal Electrode-Multilayer Ceramics Capacitor: Past, present and Future Perspectives. *Japanese Journal of Applied Physics Vol. 42*, 1-15.
- K Samuvel, K. R. (2015). Structure , Electrical and Magnetic Property investigation on Fe-doped hexagonal BaTiO₃. *Science Direct*, 356-360.
- L Singh, K.D Mandal, (2014). Effect of site on dielectric properties of Fe doped CaCu₃Ti₄O₁₂ electro-ceramic synthesized by nitrate gel route. *Indian J Phys*, 665-670.
- Zhi Yang, Y.Z (2012). Dielectric and Electrical Transport Properties of the Fe³⁺ doped CaCu₃Ti₄O₁₂. *Science Direct*, 1145-1150.

Huaiwu Zhang, Y.H (2010). Influence of temperature on dielectric properties of Fe doped $\text{CaCu}_3\text{Ti}_4\text{O}_{12}$ ceramics. *Physica B* 405, 386-389.

Bernard Durand, L.M (2007). Grain Growth-controlled Giant Permittivity in soft chemistry $\text{CaCu}_3\text{Ti}_4\text{O}_{12}$ Ceramics. *Journal of the American Ceramic Society*, Vol. 91, pp485-489.

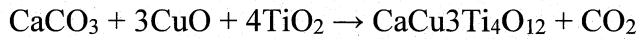
APPENDICES

APPENDIX A

Example calculation of Fe³⁺ doped CCTP ceramics for mass, lattice parameter, dielectric permittivity and dielectric loss.

Mass of 10 gram of CCTO:

Stoichiometry ratio for x = 0



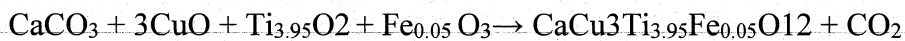
$$\text{CaCO}_3 = \frac{100.0707 \text{ g/mol} \times 10\text{g}}{658.1767 \text{ g/mol}} = 1.52 \text{ g}$$

$$3\text{CuO} = \frac{238.638 \text{ g/mol} \times 10\text{g}}{658.1767 \text{ g/mol}} = 3.63 \text{ g}$$

$$4\text{TiO}_2 = \frac{319.468 \text{ g/mol} \times 10\text{g}}{658.1767 \text{ g/mol}} = 4.85 \text{ g}$$

$$\text{Total} = 658.1767 \text{ g/mol} = 10 \text{ g}$$

Stoichiometry ratio for x = 0.05



$$\text{CaCO}_3 = \frac{100.0707 \text{ g/mol} \times 10\text{g}}{658.1767 \text{ g/mol}} = 1.47 \text{ g}$$

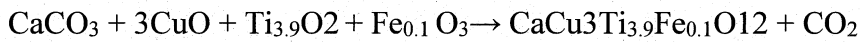
$$3\text{CuO} = \frac{238.638 \text{ g/mol} \times 10\text{g}}{658.1767 \text{ g/mol}} = 3.50 \text{ g}$$

$$3.95\text{TiO}_2 = \frac{315.47 \text{ g/mol} \times 10\text{g}}{680.97 \text{ g/mol}} = 4.63 \text{ g}$$

$$0.05\text{FeO}_3 = \frac{26.79\text{g/mol} \times 10\text{g}}{680.97\text{g/mol}} = 0.39 \text{ g}$$

$$\text{Total} = 680.97 \text{ g/mol} = 10 \text{ g}$$

Stoichiometry ratio for $x = 0.1$



$$\text{CaCO}_3 = \frac{100.07\text{g/mol} \times 10\text{g}}{679.783\text{g/mol}} = 1.46\text{ g}$$

$$3\text{CuO} = \frac{238.63\text{g/mol} \times 10\text{g}}{679.783\text{g/mol}} = 3.50\text{ g}$$

$$3.9\text{TiO}_2 = \frac{311.48\text{g/mol} \times 10\text{g}}{679.783\text{g/mol}} = 4.58\text{ g}$$

$$0.1\text{FeO}_3 = \frac{29.58\text{g/mol} \times 10\text{g}}{679.783\text{g/mol}} = 0.43\text{ g}$$

$$\text{Total} = 679.783\text{ g/mol} = 10\text{ g}$$

Example calculation of lattice parameter for doped sample $x = 0.1$ at plane (011):

$$(hkl) = (011)$$

$$n\lambda = 2d \sin\theta$$

$$1(1.5418 \text{ \AA}) = 2d \sin(14.83)$$

$$2d = 6.0238 \text{ \AA}$$

$$d = 3.012 \text{ \AA}$$

$$d(hkl) = \frac{a}{\sqrt{h^2 + k^2 + l^2}}$$

$$3.012 \text{ \AA} = \frac{a}{\sqrt{0^2 + 1^2 + 1^2}}$$

$$a = 4.26 \text{ \AA}$$

Example calculation of dielectric Permittivity for pure CCTO:

$$C_o = \epsilon_o A/t$$

$$C_o = 8.854 \times 10^{-12} / 0.021$$

$$C_o = 5.48 \times 10^{-13} \text{ F}$$

$$\epsilon = \frac{Z_i}{\omega C_o [Z_r^2 + Z_i^2]}$$

$$\epsilon = \frac{2624.71}{2(3.142)[1050.4^2 + 2624.71^2]}$$

$$\epsilon = 95.3$$

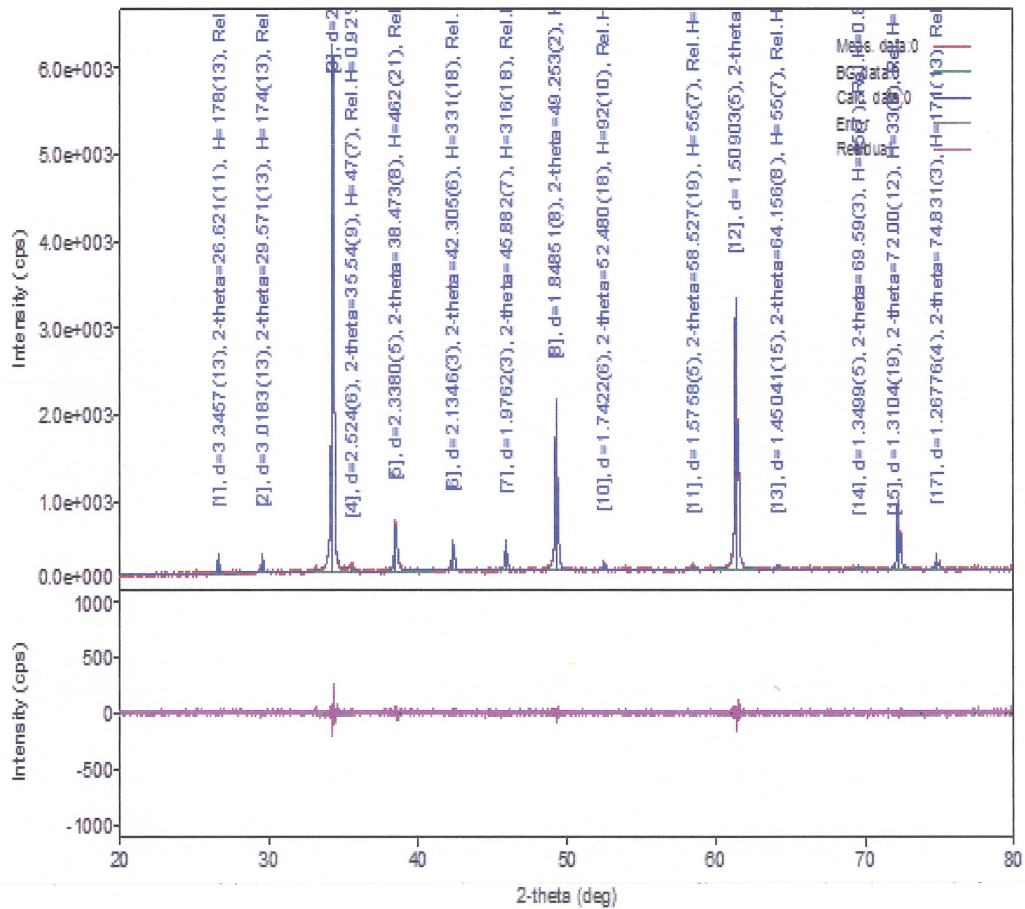
Example calculation of dielectric loss for pure CCTO:

$$\tan \epsilon = \frac{1}{2\pi f R_p C_o}$$

$$\tan \epsilon = \frac{1}{2\pi(1.0 \times 10^6 \times 369490 \times 5.481 \times 10^{-13})}$$

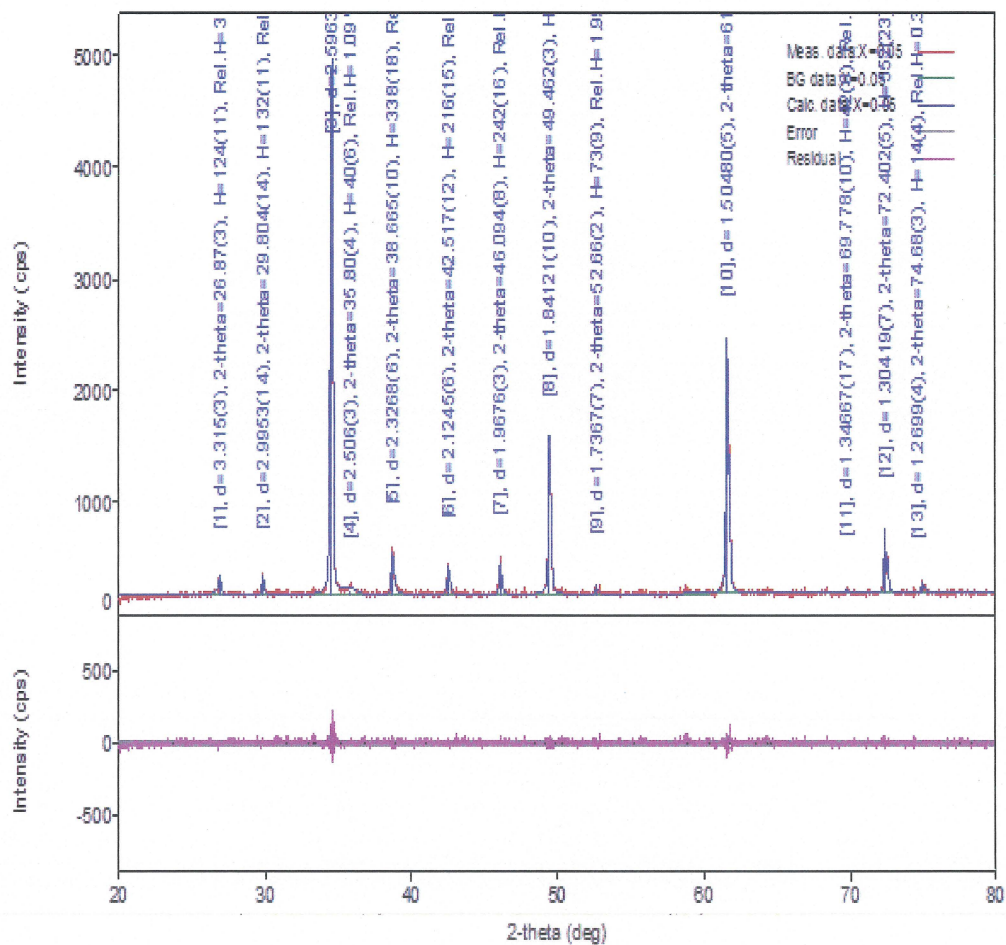
APPENDIX B

X- Ray diffraction for pure CCTO



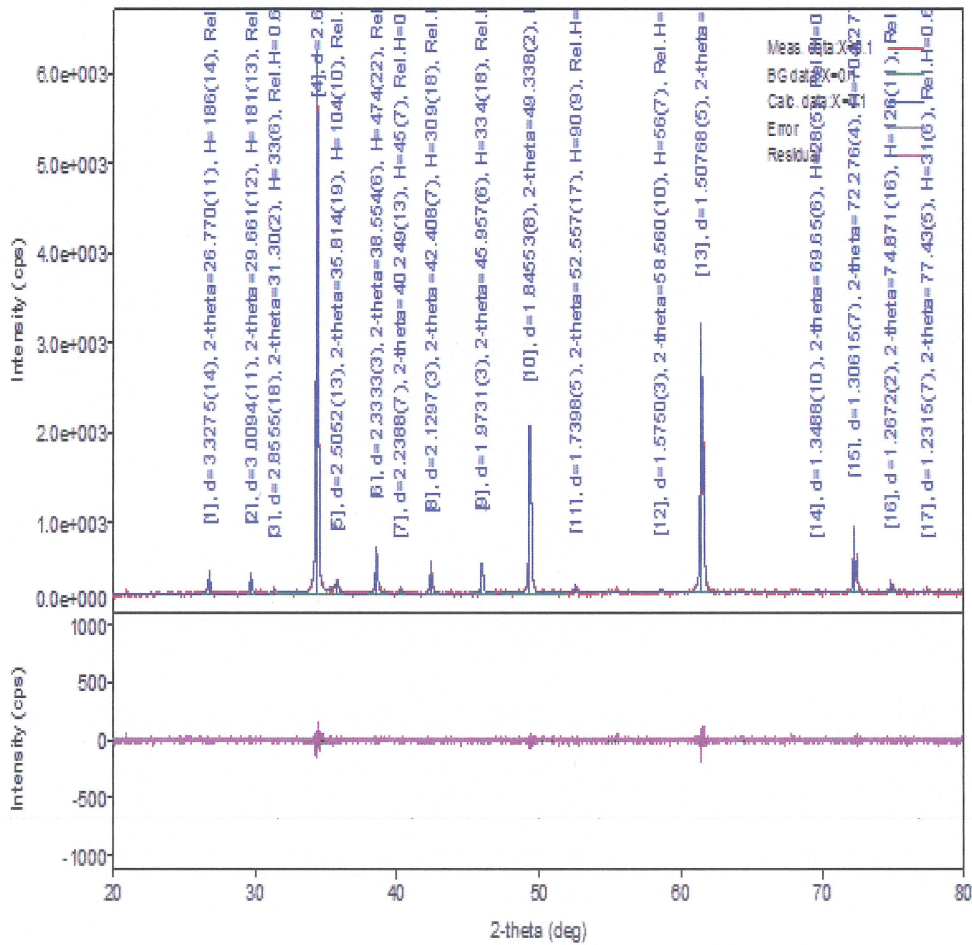
APPENDIX B

X- Ray diffraction for CCTFO $x = 0.05$



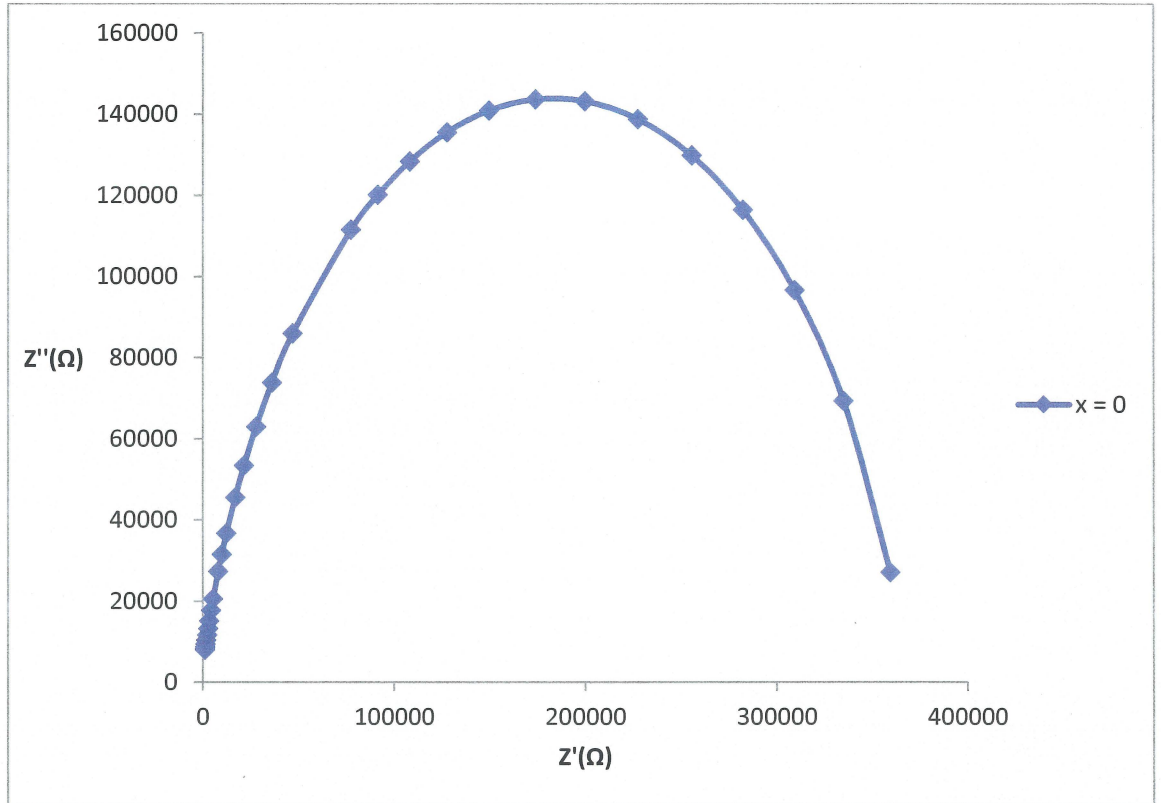
APPENDIX C

X- Ray diffraction for CCTFO $x = 0.1$



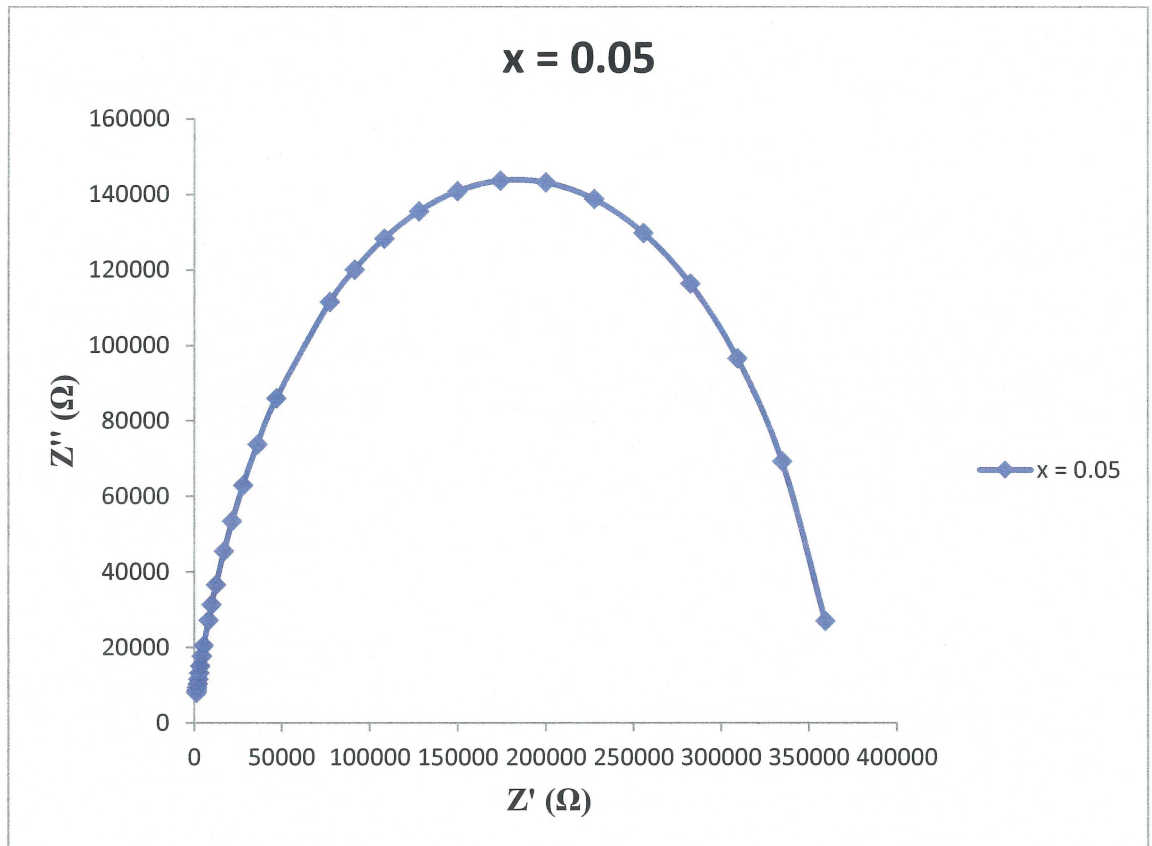
APPENDIX D

Fitted graph of pure CCTO



APPENDIX E

Fitted graph of CCTFO with $x = 0.05$



APPENDIX F

Fitted graph of CCFTO with $x = 0.1$

